J Mater Sci (2006) 41:4706–4712
DOI 10.1007/s10853-006-0045-4

Magnetization study of Fe-doped ZnO co-doped with Cu: Synthesized by wet chemical method

O. D. Jayakumar · I. K. Gopalakrishnan · S. K. Kulshreshtha

Received: 15 June 2005 / Accepted: 23 September 2005 / Published online: 4 May 2006

Abstract Fe- and Cu-doped ZnO of nominal compositions $Zn_{0.95}Fe_{0.05}O$ and $Zn_{0.94}Fe_{0.05}Cu_{0.01}O$ were synthesized by a wet chemical route. X-ray diffraction analysis of the samples annealed at 575 K showed that they are single phase without any secondary phases. *DC* magnetization measurements of Cu co-doped samples ($Zn_{0.94}Fe_{0.05}Cu_{0.01}O$) as a function of field at room temperature showed ferromagnetic signature while the samples without Cu co-doping ($Zn_{0.95}Fe_{0.05}O$) are paramagnetic in nature. On increasing the temperature of annealing from 575 K to 1,075 K an impurity phase emerges in both the samples, which has been identified as a variant of $ZnFe_2O_4$. Both the samples heated at and above 1,075 K are found to be paramagnetic at room temperature. These observations, the absence of room temperature ferromagnetism in $Zn_{0.95}Fe_{0.05}O$ and the disappearance of ferromagnetism in $Zn_{0.94}Fe_{0.05}Cu_{0.01}O$ on raising the temperature of annealing clearly rules out the likelihood of room temperature ferromagnetism arising from the impurity phases like γ-Fe_2O_3 and/or $ZnFe_2O_4$ that might have been formed during the synthesis. Our results strongly suggest that room temperature ferromagnetism in $Zn_{0.94}Fe_{0.05}Cu_{0.01}O$ can be attributed to the formation of a secondary phase of Cu-doped $ZnFe_2O_4$.

Introduction

Dilute magnetic semiconductors (DMSs) have attracted considerable amount of attention after the theoretical work by Dietl et al. [1] predicted room temperature ferromagnetism in them. DMSs are expected to play an important role in multidisciplinary materials science and future spintronics because both charge and spin degrees of freedom are accommodated into single matter and their interplay is expected to explore novel physics and new devices [2]. The use of carrier spin, in addition to charge, appears promising for a new class of devices such as spin light emitting diodes, spin field-effect transistors and spin qubits for quantum computers. The introduction of substitutional transition metal (TM) dopants into wide band gap oxides and III–V semiconductors has been shown to induce carrier-induced ferromagnetism [3, 4]. Ferromagnetism in these materials operates via a mechanism by which the itinerant carriers are spin polarized and mediate the ferromagnetic ordering between the widely spaced dopant ions (RKKY interaction) when the localized spin is introduced into the oxide semiconductor. Such long-range ferromagnetic ordering demands materials with high structural quality. Recently double exchange interaction has also been proposed as an alternative mechanism in Fe-doped ZnO co-doped with Cu [5, 6]. More recently, Coey et al. [7] have proposed donor impurity band exchange in DMS oxides. According to their model ferromagnetic exchanges in DMS oxides are mediated by shallow donor electrons that form bound magnetic polarons, which overlap to create a spin-split impurity band. TM-doped ZnO has been the main workhorse for the researchers looking for DMS having room temperature ferromagnetism [8–16]. ZnO is an optically transparent wide gap semiconductor (E_g~3.44 eV) with exciton binding energy of ~60 meV. However, experimental results on the TM-doped ZnO do not converge on an explicit conclusion. Often contradicting reports by different groups lead to the debate whether the system shows room temperature ferromagnetism at all, and in case it does, is it intrinsic to the

O. D. Jayakumar · I. K. Gopalakrishnan (✉) · S. K. Kulshreshtha
Chemistry Division, Bhabha Atomic Research Centre, Mumbai 400 085, India
e-mail: ikgopal@magnum.barc.ernet.in

materials [8–16]. Majority of the groups observed ferromagnetism only at low temperatures. This has been attributed to the clustering of magnetic ions and impurity phases [8–12]. There are few reports about the observance of room temperature ferromagnetism in thin films made under nonequilibrium conditions. Recently, Han et al. [16, 17] observed room temperature ferromagnetism in Fe-doped ZnO co-doped with Cu in bulk samples prepared by high temperature solid-state reaction. Bulk samples have the advantage of insensitivity to the detailed process conditions, compared to the films fabricated under nonequilibrium conditions. Sharma et al. [15] also observed room temperature ferromagnetism in bulk Mn-doped ZnO synthesized by the solid-state reaction of ZnO with MnO_2 at low temperatures. They have also found that on heating the bulk samples above 875 K ferromagnetic content of the sample decreases, which they attributed to the clustering of Mn. All these observations points to the fact that the success of sample preparation, showing room temperature ferromagnetism, depends not only on the precise details and route but also on the quality of starting materials used. The oxidation state (and spin state), homogeneity and the substitutional incorporation of the dopants must be considered when the TM is doped for producing DMSs. Heating the sample increases the possibility of inadvertently altering the oxidation state of the dopants [18]. This motivated us to synthesize Fe-doped ZnO co-doped with Cu by a wet chemical method since one can obtain more homogenous product by this route at a relatively lower temperature [19]. This paper describes our efforts in synthesizing nanocrystalline samples having room temperature ferromagnetic characteristics by incorporating Fe and Cu in ZnO. Our study indicates that the observed room temperature ferromagnetism can be due to the formation of a secondary phase $Zn_{1-x}Cu_xFe_2O_4$ rather than due to the incorporation of TM ions into ZnO lattice.

Experimental

$Zn_{0.94}Fe_{0.05}Cu_{0.01}O$ and $Zn_{0.95}Fe_{0.05}O$ nanocrystallites were synthesized by co-precipitation method using aqueous solutions of zinc acetate di hydrate (purity 99.99%), cupric acetate monohydrate (purity 99.99%), ammonium ferrous sulphate (purity 99.98%) and potassium hydroxide. Two aqueous solutions, one containing zinc acetate, cupric acetate and ammonium ferrous sulphate and other containing KOH in appropriate proportion were prepared by vigorous magnetic stirring for 2 h. The KOH solution was added to the solution containing zinc acetate, cupric acetate and ammonium ferrous sulphate while stirring and the yellow precipitate formed was separated from the solution by filtration. The filtrate was washed several times using distilled water and absolute ethanol to remove the impurities like sulphate and potassium ions and subsequently dried in an oven for 16 h at 400–425 K. The nanocrystalline samples were obtained by annealing the oven-dried particles at 575 K while bulk samples by annealing at 1,075 K for 6 h. The compounds $ZnFe_2O_4$ and $Zn_{0.6}Cu_{0.4}Fe_2O_4$ were also prepared by the same method. The Phase purity and the structure of the samples were analysed using Ni filtered CuKα radiation by employing a Philips Diffractometer (model PW 1071) fitted with graphite crystal monochromater. The lattice parameters of the compounds were extracted by Rietveld refinement of the XRD data by using the program Fullprof [20] with X-ray intensity collected for the range $10° \leq 2\theta \leq 70°$. Average crystallite size was determined from the extra broadening of the X-ray diffraction (XRD) peaks of the sample using Scherrer's formula applied to the strongest peak. *DC* magnetization measurements as a function of temperature and field were carried out using an E.G.&G P.A.R vibrating sample magnetometer (model 4500).

Results and discussion

The Rietveld refinement analysis of XRD data of $Zn_{0.95}Fe_{0.05}O$ and $Zn_{0.94}Fe_{0.05}Cu_{0.01}O$ samples annealed at 575 K and 1,075 K are presented in Fig. 1. In addition, the pristine ZnO prepared by the same method is also given for comparison. Dots correspond to the data and solid lines through the points are the results of Rietveld analysis. Vertical tics below the curve *a* indicate expected peak positions for the wurtzite phase while that below the curve *d* indicate that of spinel $(Cu,Zn)Fe_2O_4$ phase which emerges in the samples when the annealing temperature was raised to 1,075 K. The Rietveld analysis provided convincing evidence that the samples are single phase when the temperature of annealing was limited to 575 K. Due to the poor contrast between Fe, Cu and Zn in XRD the analysis could not be used to refine the relative amounts of these ions in the wurtzite structure. However, Rietveld analysis allowed the extraction of accurate cell parameters.

It can be seen that all the peaks in both $Zn_{0.94}Fe_{0.05}Cu_{0.01}O$ and $Zn_{0.95}Fe_{0.05}O$ could be fitted with wurtzite structure conforming to the space group $P6_3mc$ (No.186). It can also be seen that both samples ($Zn_{0.94}Fe_{0.05}Cu_{0.01}O$ and $Zn_{0.95}Fe_{0.05}O$) annealed at 575 K have very broad peaks due to their nanocrystalline nature. It is worth noting that even though all samples were prepared by the same method, $Zn_{0.95}Fe_{0.05}O$ have broadest peaks as compared to

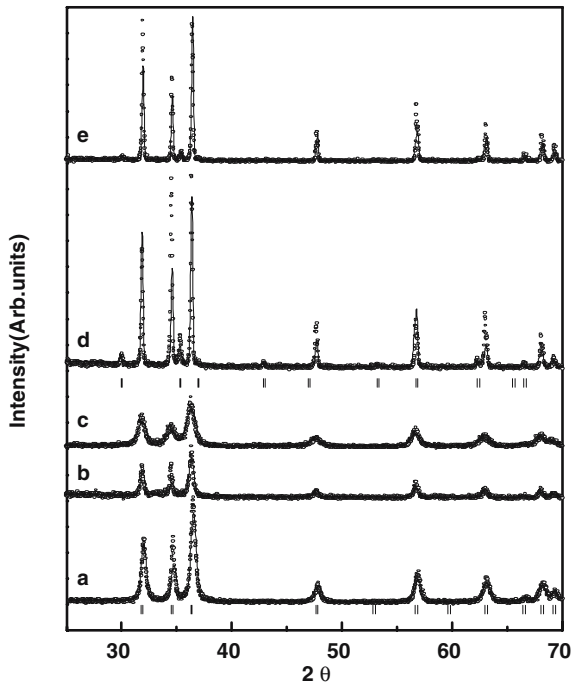

Fig. 1 Rietveld refinement profiles of XRD data (room temperature) of $Zn_{0.95}Fe_{0.05}O$ and $Zn_{0.94}Fe_{0.05}Cu_{0.01}O$ nanocrystallites annealed at 575 K and bulk samples annealed at 1,075 K. XRD of pristine ZnO annealed at 575 K is also shown for comparison. (**a**) ZnO—575 K, (**b**) $Zn_{0.94}Fe_{0.05}Cu_{0.01}O$—575 K, (**c**) $Zn_{0.95}Fe_{0.05}O$–575 K, (**d**) $Zn_{0.95}Fe_{0.05}O$–1,075 K and (**e**) $Zn_{0.94}Fe_{0.05}Cu_{0.01}O$—1,075 K. The vertical tics below the curve *a* indicate the allowed reflections for wurtzite phase while that below the curve *d* indicate that of cubic spinel

$Zn_{0.94}Fe_{0.05}Cu_{0.01}O$ and ZnO. The crystallite size of samples, annealed at 575 K, as determined from the extra broadening of diffraction peaks using Scherrer's formula is ~10 nm and ~19 nm for $Zn_{0.95}Fe_{0.05}O$ and $Zn_{0.94}Fe_{0.05}Cu_{0.01}O$ respectively. However, on raising the temperature of annealing to 1,075 K an impurity phase emerges in both the samples. We have identified all the impurity lines to that of spinel compound with cubic symmetry (space group Fd3m). Thus, in the case of samples annealed at 1,075 K Rietveld refinement analysis involved fitting two crystalline phases, wurtzite and spinel. Lattice parameters of all the samples extracted from the Rietveld analysis are presented in Table 1. The value of lattice parameter '*a*' of impurity phase in $Zn_{0.95}Fe_{0.05}O$ is 8.413(2) Å while its value in $Zn_{0.94}Fe_{0.05}Cu_{0.01}O$ is 8.414(2) Å. This value is closer to the lattice parameter reported in the literature for $ZnFe_2O_4$ and $(Zn,Cu)Fe_2O_4$ [21]. Hence it is reasonable to assume that the impurity phase as Cu-doped Zn-ferrite ($Zn_{1-x}Cu_xFe_2O_4$ ($0.0 \leq x \leq 0.4$)).

DC Magnetization data of $Zn_{0.94}Fe_{0.05}Cu_{0.01}O$ annealed at 575 K, is presented in Fig. 2. It can be seen that the magnetization loops of $Zn_{0.94}Fe_{0.05}Cu_{0.01}O$ recorded at room temperature and 5 K are ferromagnetic in nature. For $Zn_{0.94}Fe_{0.05}Cu_{0.01}O$ there is rapid increase in magnetization at lower fields that saturates at higher fields indicating its ferromagnetic nature. However, there is no hysteresis and little remanence for the loop recorded at room temperature (inset at top left corner). This can be attributed to its particle size, which is in the nanophase regime. It can be seen that *M–H* loop recorded at 5 K shows clear hysteresis as compared to that recorded at room temperature. It is a highly symmetrical hysteresis loop with a coercive field of 600 Oe and remanence of 0.1 emu/g. This shows that the sample gets stabilized in the ferromagnetic state as temperature is lowered as is expected of any nanostructured magnetic materials. The temperature dependence of the magnetization (inset at bottom right corner), under the *ZFC* and *FC* mode, gives further confirmation of this transition from superparamagnetic to ferromagnetic state. Nevertheless, the value of saturation magnetization (M_s) is only 0.423 emu/g (Fig. 3). This corresponds to 0.124 μ_B/Fe^{2+} ion. This value of M_s is far below the full moment of Fe^{2+}-ion. This indicates only a small fraction of the substituted Fe is participating in the long-range order.

In Fig. 3 we have presented *DC* magnetization data of $Zn_{0.94}Fe_{0.05}Cu_{0.01}O$ (annealed at 1,075 K). It can be seen from *M–H* loop recorded at room temperature that it is paramagnetic. Its *M–T* plot at an applied field of 1,000 Oe is shown in the inset. It can be seen that both *ZFC* and *FC*

Table 1 Lattice parameters of different samples with varying thermal treatments

Sample composition	Wurtzite phase space group: P63mc		Cubic spinel space group: Fd3m
	a (Å)	*c* (Å)	*a* (Å)
$Zn_{0.95}Fe_{0.05}O$ (575 K)	3.250(1)	5.207(1)	Not detectable
$Zn_{0.95}Fe_{0.05}O$ (1,075 K)	3.2509(6)	5.1988(8)	8.413(2)
$Zn_{0.94}Fe_{0.05}Cu_{0.01}O$ (575 K)	3.247(1)	5.203(2)	Not detectable
$Zn_{0.94}Fe_{0.05}Cu_{0.01}O$ (1,075 K)	3.2436(6)	5.1987(8)	8.414(2)
$ZnFe_2O_4$ (575 K)			8.450(9)
$ZnFe_2O_4$ (1,075 K)			8.462(3)
$Zn_{0.6}Cu_{0.4}Fe_2O_4$ (575 K)			8.343(9)
$Zn_{0.6}Cu_{0.4}Fe_2O_4$ (1,075 K)			8.447(2)
ZnO + $Zn_{0.6}Cu_{0.4}Fe_2O_4$ (575 K)	3.246(1)	5.201(1)	
ZnO + $Zn_{0.6}Cu_{0.4}Fe_2O_4$ (1,075 K)	3.2472(4)	5.2008(5)	8.434(2)

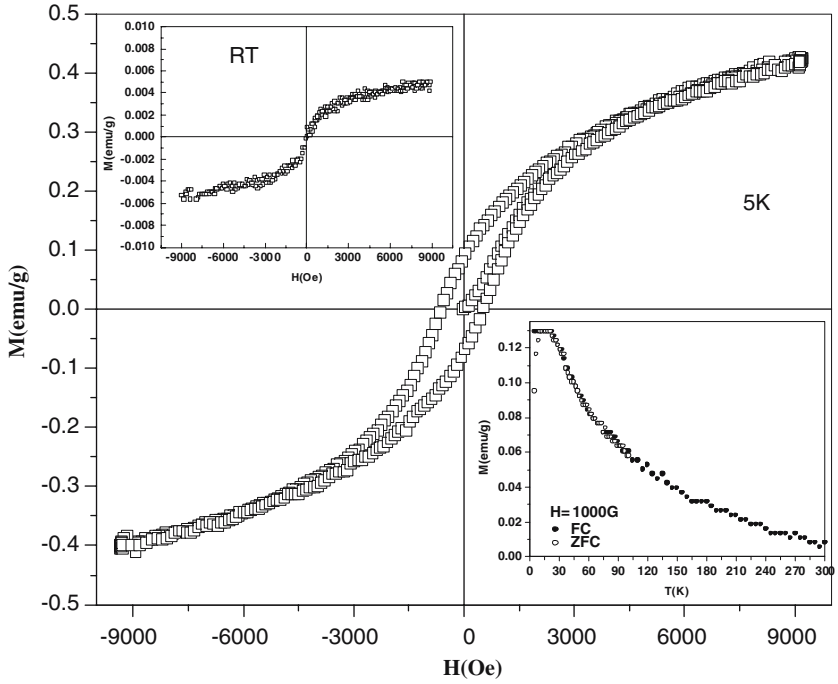

Fig. 2 Isothermal magnetization of $Zn_{0.94}Fe_{0.05}Cu_{0.01}O$ sample annealed at 575 K recorded at 5 K and at room temperature (inset in the top left corner). Magnetization data as a function of temperature for $Zn_{0.94}Fe_{0.05}Cu_{0.01}O$ annealed at 575 K is given in the inset (right bottom corner). Both *ZFC* and *FC* plots are presented. Open symbols correspond to *ZFC* data while closed symbols indicate *FC* data.

plots of $Zn_{0.94}Fe_{0.05}Cu_{0.01}O$ (annealed at 1,075 K) go through a maximum as the temperature is lowered indicating spin glass like behaviour. In addition, its *M–H* loop at 5 K showed lack of hysteresis and non-linearity. Such behaviour is typical of spin glasses [22]. This shows that on annealing $Zn_{0.94}Fe_{0.05}Cu_{0.01}O$ at higher temperatures magnetic ions probably gets clustered indicating the instability of Fe-doped ZnO. Similar behaviour has been reported in literature [8–12, 15]. Figure 4 depicts *M–H* loops of $Zn_{0.95}Fe_{0.05}O$ (annealed at 575 K) and recorded at 295, 205, 105 and 5 K. It can be seen that *M–H* loops at 295 and 205 K are linear while that recorded at 105 and 5 K are *S* shaped without any hysteresis. Lack of hysteresis can be attributed to the particle size effect. This indicates that paramagnetic to superparamagnetic transition in $Zn_{0.95}Fe_{0.05}O$ (annealed at 575 K) takes place below 205 K. This is supported by the *M–T* plots at an applied field of 100 Oe, depicted in the inset. There is hardly any difference between ZFC and FC plots down to 5 K.

The absence of room temperature ferromagnetism in $Zn_{0.95}Fe_{0.05}O$ indicates that the observed ferromagnetism in $Zn_{0.94}Fe_{0.05}Cu_{0.01}O$ is not due to any impurity phases like $ZnFe_2O_4$ or γ-Fe_2O_3 formed during its synthesis. The disappearance of ferromagnetism in $Zn_{0.94}Fe_{0.05}Cu_{0.01}O$ on annealing the sample at higher temperature also indicates that the observed room temperature ferromagnetism in this sample cannot be attributed to the formation of small amount of $CuFe_2O_4$. Thus it is tempting to attribute the observed ferromagnetism to the incorporation of Fe and Cu in to the ZnO lattice. However, it is worth noting that the magnetization value of ferromagnetic $Zn_{0.94}Fe_{0.05}Cu_{0.01}O$ (Fig. 2) is smaller than that observed for the paramagnetic one (Fig. 3). This is contrary to what is generally observed. This anomalous behaviour points to the possibility that the observed ferromagnetism in $Zn_{0.94}Fe_{0.05}Cu_{0.01}O$ is likely to arise from the formation of secondary phases. It is possible that the amount of the ferromagnetic impurity phase formed at low temperature treated sample is insignificant as compared to the paramagnetic impurity phase formed by the high temperature treatment. One impurity phase that can be

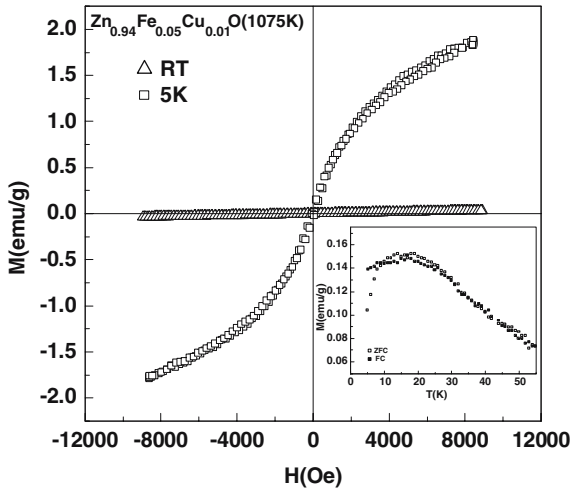

Fig. 3 Isothermal magnetization of $Zn_{0.94}Fe_{0.05}Cu_{0.01}O$ annealed at 1,075 K and recorded at RT and 5 K. Inset shows their magnetization data as a function of temperature at an applied field of 1,000 Oe. Both *ZFC* and *FC* plots are given. Open symbols correspond to *ZFC* data while closed symbols indicate *FC* data

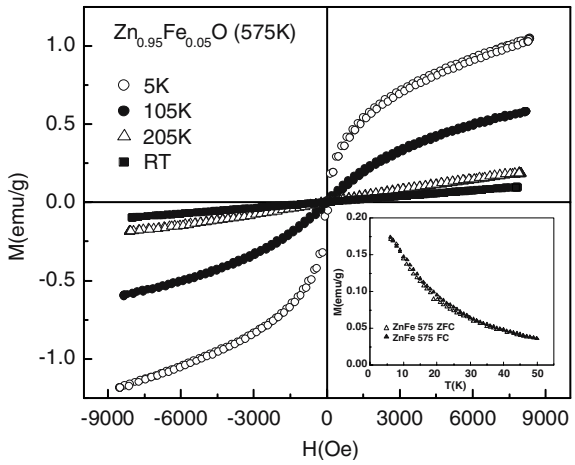

Fig. 4 Isothermal magnetization of $Zn_{0.95}Fe_{0.05}O$ annealed at 575 K and generated at different temperatures. Magnetization data as a function of temperature for $Zn_{0.95}Fe_{0.05}O$ (annealed at 575 K) is given in the inset

the source of room temperature ferromagnetism in these samples is Cu-doped Zn-ferrite. Ideal zinc ferrite ($ZnFe_2O_4$) is a normal spinel where zinc cations occupy all of the tetrahedral sites and iron ions are on the octahedral sites. In the bulk material there are rather weak magnetic intra sublattice interactions between moments of octahedrally coordinated Fe^{3+} cations generating long-range antiferromagnetic order below 10 K [23]. On the other hand, the nanostructured compound with high degree of inversion orders ferrimagnetically at temperature as high as 500 K [24]. Such effects have been associated to the presence of Fe^{3+} ions at the tetrahedral sites and the consequent existence of non-zero exchange interactions between iron cations on different sites [25]. This process of partial inversion is strongly dependent on the method employed to prepare $ZnFe_2O_4$ nanostructured materials [26, 27]. Methods which use high temperature treatment generally lead to an ideal normal spinel structure where as high energy ball milling [27, 28] and soft chemical routes, such as hydrothermal and co-precipitation [25, 26] or reverse micelle synthesis [29], induce a certain degree of inversion. Ferrimagnetism in $ZnFe_2O_4$ can also be induced by partially substituting Zn by Cu [21]. $ZnFe_2O_4$ prepared by us did not show any ferrimagnetism at room temperature. However, there is a possibility that the observed room temperature ferromagnetism in $Zn_{0.94}Fe_{0.05}Cu_{0.01}O$ can be due to $(Zn,Cu)Fe_2O_4$. XRD patterns of both samples ($Zn_{0.95}Fe_{0.05}O$ and $Zn_{0.94}Fe_{0.05}Cu_{0.01}O$) heated at 1,075 K, depicted in Fig. 1, clearly showed the presence of an impurity phase that has been identified as a cubic spinel with lattice parameters closer to $ZnFe_2O_4$. In order to elucidate this point we have synthesized $ZnFe_2O_4$ and $Zn_{0.6}Cu_{0.4}Fe_2O_4$ (this composition was arrived at by taking into account the amount of Cu and Fe that has been incorporated into $Zn_{0.94}Fe_{0.05}Cu_{0.01}O$) by the same method used for preparing Fe- and Cu-doped ZnO samples. X-ray Rietveld refinement profiles of $ZnFe_2O_4$ annealed at 575 K and $Zn_{0.6}Cu_{0.4}Fe_2O_4$ annealed at 575 K and 1,075 K are presented in Fig. 5. It can be seen from Fig. 5 that all compounds can be fitted as cubic spinel structure. Lattice parameters extracted from the refinement are presented in Table 1. *DC* magnetization loops generated at room temperature on $ZnFe_2O_4$ annealed at 575 K and $(Zn_{0.6}Cu_{0.4})Fe_2O_4$ annealed at 575 K and 1,075 K are presented in Fig. 6. It can be seen that $ZnFe_2O_4$ is paramagnetic while $(Zn_{0.6}Cu_{0.4})Fe_2O_4$ is ferromagnetic in nature. The presence of ferromagnetic signal, at room temperature, in $(Zn_{0.6}Cu_{0.4})Fe_2O_4$ suggests that this impurity phase can be the source for the observed room temperature ferromagnetism in $Zn_{0.94}Fe_{0.05}Cu_{0.01}O$. However, on annealing

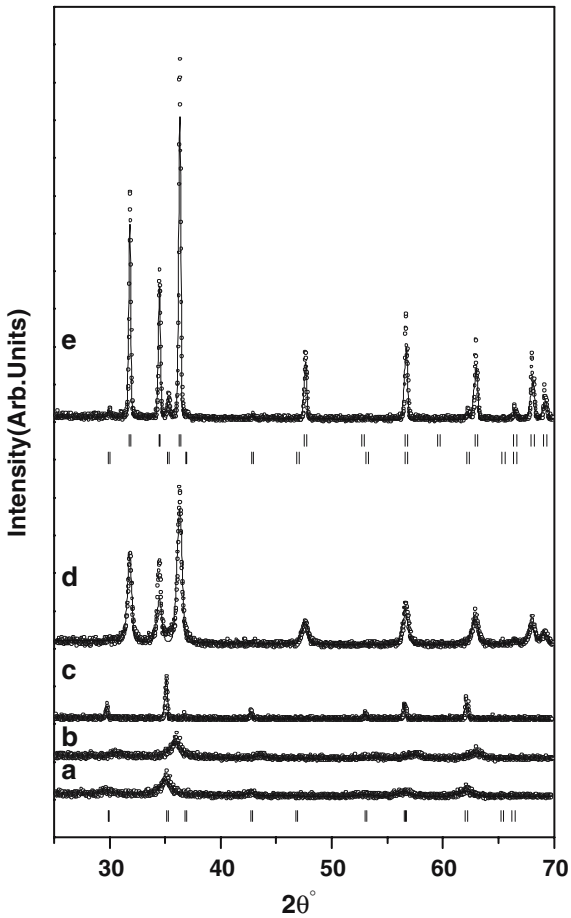

Fig. 5 Rietveld refinement profiles of XRD data (room temperature) of $ZnFe_2O_4$, $Zn_{0.6}Cu_{0.4}Fe_2O_4$ and mixed phase sample (ZnO + $(Zn_{0.6}Cu_{0.4})Fe_2O_4$) annealed at 575 K and 1,075 K. (**a**) $ZnFe_2O_4$—575 K, (**b**) $Zn_{0.6}Cu_{0.4}Fe_2O_4$—575 K, (**c**) $Zn_{0.6}Cu_{0.4}Fe_2O_4$—1,075 K, (**d**) mixed phase sample (ZnO + $(Zn_{0.6}Cu_{0.4})Fe_2O_4$) annealed at 575 K and (**e**) mixed phase sample (ZnO + $(Zn_{0.6}Cu_{0.4})Fe_2O_4$) annealed at 1,075 K. The vertical tics below the curve *a* indicate the allowed reflections for cubic spinel while that below the curve *e* indicate that of wurtzite and spinel (lower tics)

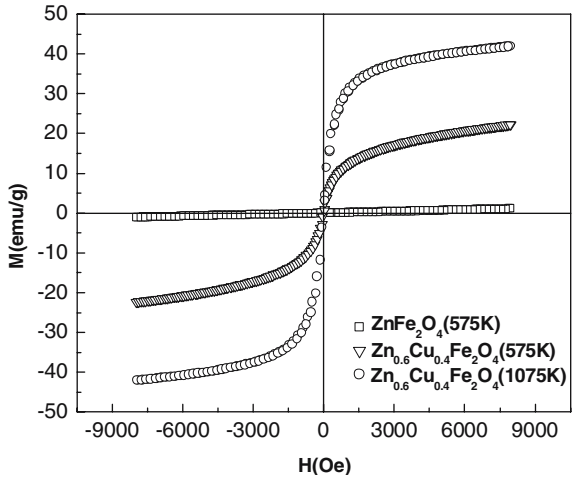

Fig. 6 Magnetization data for $ZnFe_2O_4$ annealed at 575 K and $(Zn_{0.6}Cu_{0.4})Fe_2O_4$ annealed at 575 K and 1,075 K

$(Zn_{0.6}Cu_{0.4})Fe_2O_4$ at 1,075 K its saturation magnetization increases. This is contrary to what was observed in $Zn_{0.94}Fe_{0.05}Cu_{0.01}O$. $Zn_{0.94}Fe_{0.05}Cu_{0.01}O$ became paramagnetic when it was annealed at 1,075 K. This may be due to the decrease of Cu content in $(Zn_{1-x}Cu_x)Fe_2O_4$ on annealing it in the ZnO environment at 1,075 K. In order to clarify this point we have prepared a mixed phase sample by mixing as prepared ZnO and $Zn_{0.6}Cu_{0.4}Fe_2O_4$ in the ratio 92.5:2.5. This ratio was arrived at by assuming that the entire amount of Cu and Fe doped into ZnO reacted to form CuZn-ferrite. These mixtures were then annealed at 575 K and 1,075 K for the same duration as was done for the Fe- and Cu-doped ZnO samples. XRD patterns of the mixture of ZnO + $Zn_{0.6}Cu_{0.4}Fe_2O_4$ (herein after called mixed phase sample) annealed at 575 K and 1,075 K are presented in Fig. 5. It can be seen that the XRD patterns of mixed phase samples annealed at 575 K and 1,075 K looks similar to that of $Zn_{0.94}Fe_{0.05}Cu_{0.01}O$. It is worth noting that the mixed phase sample annealed at 575 K apparently did not show any peaks corresponding to $Zn_{0.6}Cu_{0.4}Fe_2O_4$. The absence of any peaks corresponding to $Zn_{0.6}Cu_{0.4}Fe_2O_4$ can be due to its low concentration and its nanocrystalline nature. This is also evident from the XRD patterns of $ZnFe_2O_4$ and $Zn_{0.6}Cu_{0.4}Fe_2O_4$ annealed at 575 K. In view of the above observations it is reasonable to assume that the peaks due to $Zn_{0.6}Cu_{0.4}Fe_2O_4$ in the mixed phase sample are masked by the background radiation of the XRD pattern of ZnO. This explains the absence of any peaks due to $(Cu,Zn)Fe_2O_4$-ferrite in the XRD pattern of $Zn_{0.94}Fe_{0.05}Cu_{0.01}O$ annealed at 575 K presented in Fig. 1. It can be seen that the XRD patterns of $Zn_{0.94}Fe_{0.05}Cu_{0.01}O$ and the mixed phase samples are similar. Lattice parameters of mixed phase sample are listed in Table 1. The room temperature magnetization loops of mixed phase sample annealed at 575 K and 1,075 K are presented in Fig. 7. It can be seen that mixed phase sample annealed at 575 K is ferromagnetic while that annealed at 1,075 K is paramagnetic. These observations clearly suggest that the origin of room temperature ferromagnetism in Fe- and Cu-doped ZnO samples, prepared by the wet chemical method, can be attributed to the formation of an impurity phase of Cu-doped $ZnFe_2O_4$ rather than due to the carrier-induced ferromagnetism [3, 4] or double exchange interaction [5, 6] as proposed by different groups. Han et al. have observed room temperature ferromagnetism in $Zn_{0.94}Fe_{0.05}Cu_{0.01}O$ prepared by solid-state reaction of ZnO, FeO and CuO at 1,170 K. However, our samples lost ferromagnetic characteristic by annealing them at 1,075 K. This again points to the dependence of sample preparation route and the quality and nature of starting materials in obtaining room temperature ferromagnetism in TM-doped ZnO.

Conclusions

We have synthesized Fe-doped ZnO with and without Cu co-doping by a wet chemical method followed by annealing them at different temperatures. Rietveld Profile refinement analysis and powder XRD data of low temperature annealed (575 K) samples showed the formation of a single-phase compound with wurtzite structure. However, XRD patterns of high temperature annealed samples showed the presence of an impurity phase, which has been identified as a variant of $ZnFe_2O_4$. The apparent absence of this phase in the samples annealed at 575 K may be due to the broadness of impurity phase peaks, the low level of dopant concentration and the lack of its crystallinity. A detailed analysis of XRD and *DC* magnetization data strongly suggest that the room temperature ferromagnetism observed in $Zn_{0.94}Fe_{0.05}Cu_{0.01}O$,

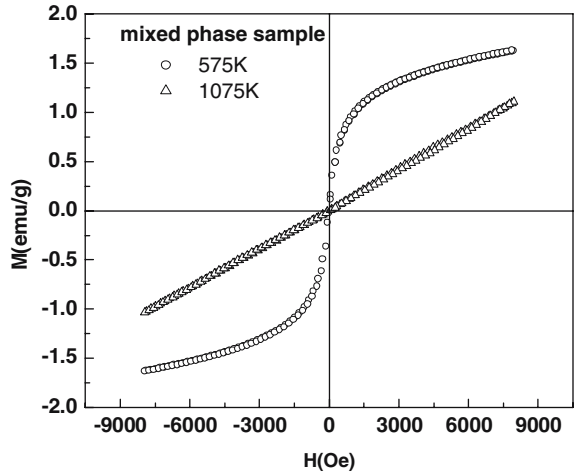

Fig. 7 Magnetization data for mixed phase sample (ZnO + $(Zn_{0.6}Cu_{0.4})Fe_2O_4$) annealed at 575 K and 1,075 K

prepared by us by the wet chemical method, can be attributed to the formation of an impurity phase of $Zn_{1-x}Cu_xFe_2O_4$ ($0 \leq x \leq 0.4$) rather than due to the incorporation of TM ions (Fe and Cu) into ZnO lattice.

References

1. Dietl T, Ohno H, Matsukura, F, Cibert J, Ferrand D (2000) Science 287:1019
2. Wolf SA, Awschalom DD, Buhrman RA, Daughton JM, von Molnar S, Roukes ML, Chtchelkanova AV, Treger DM (2001) Science 294:1488
3. Ohno Y, Young DK, Beshoten B, Matsukura F, Ohno H, Awschalom DI (1999) Nature 402:790
4. Pearton SJ, Abernathy CR, Overberg ME, Thaler GT, Nortan DP, Theodorpoulou N, Hebard AF, Park YD, Ren F, Kim J, Boatner LA (2003) J Appl Phys 93:1
5. Park MS, Min BI (2001) Phys Rev B 308–310:904
6. Park MS, Min BI (2003) Phys Rev B 68:224436
7. Coey JMD, Venkatesan M, Fitzgerald CB (2005) Nat Mater 4:173
8. Jeonga YH, Hana S-J, Parka J-H, Lee YH (2004) J Magn Magn Mater 272–276:1976
9. Jin Z, Fukumura T, Kawasaki M, Ando K, Saito H, Sekiguchi T, Yoo YZ, Murakami M, Matsumoto Y, Hasegawa T, Koinuma H (2001) Appl Phys Lett 78:3824
10. Ueda K, Tabata H, Kawai T (2001) Appl Phys Lett 79:988
11. Jung SW, An SJ, Yi GC, Jung CU, Lee SI, Cho S (2002) Appl Phys Lett 80:4561
12. Fukumura T, Jin Z, Kawasaki M, Shono T, Hasegawa T, Koshihara S, Koinuma H (2001) Appl Phys Lett 78:958
13. Cheng XM, Chien CL (2003) J Appl Phys 93:7876
14. Yoon SW, Cho SB, We SC, Yoon S, Suh BJ, Song HK, Shin YJ (2003) J Appl Phys 93:7879
15. Sharma P, Gupta A, Rao KV, Owens FJ, Sharma R, Ahuja R, Osorio Gillen JM, Johasson B, Gehring GA (2003) Nat Mater 2:673
16. Han SJ, Song JW, Yang CH, Park SH, Park JH, Jeong YH, Rhie KW (2002) Appl Phys Lett 81:4212
17. Han S-J, Jang T-H, Kim YB, Park BG, Park J-H, Jeong YH (2003) Appl Phys Lett 83:920
18. Kundaliya DC, Ogale SB, Lofland SE, Dhar S, Metting CJ, Shinde SR, Ma Z, Varughese B, Ramanujachary KV, Salamanca-Riba L, Venkatesan T (2004) Nat Mater 3:709
19. Norberg NS, Kittilstved KR, Amonette JE, Kukkadapu RV, Schwartz DA, Gamelin DR (2004) J Am Chem Soc 126:9387
20. Rodriguez-Carvajal J Fullprof: a program for Rietveld refinement and profile matching analysis of complex powder diffraction patterns ILL
21. Rana MU, Misbah-ul I, Tahir A (2000) Mater Chem Phys 65:345
22. Hurd CM (1982) Contemp Phys 23:469
23. Burghart FJ, Potzel W, Kalvius GM, Schreier E, Grosse G, Noakes DR, Schafer W, Kockelmann W, Campbell SJ, Kaczmarek WA, Martin A, Krause MK (2000) Physica B 289–290:286
24. Schafer W, Kockelmann W, Kirfel A, Potzel W, Burghart FJ, Kalvius GM, Martin A, Kaczmarek WA, Schreier E, Campbell SJ (2000) Mater Sci Forum 321–324:802
25. Goya GF, Rechenberg HR (1999) J Magn Magn Mater 196–197:191
26. Schiessl W, Potzel H, Karzel M, Steiner GM, Kalvius A, Martin MK, Halevy I, Gal J, Schäfer W, Will G, Hillberg M, Wäppling R (1996) Phys Rev B 53:9143
27. Guaiata FJ, Beltrán H, Cordoncillo E, Carda JB, Escribano P (1999) J Eur Ceram Soc 19:363
28. Hamdeh H, Ho JC, Oliver SA, Willey RJ, Oliveri G, Busca GJ (1997) J Appl Phys 81:1851
29. Hochepied JF, Bonville P, Pilen MP (2000) J Phys Chem B 104:5